Modeling flank wear of carbide tool insert in metal cutting

X. Luo[1*], K. Cheng[1], R. Holt[1] and X. Liu[2]

[1]School of Technology, Leeds Metropolitan University, Calverley Street, Leeds, LS1 3HE, UK

[2]School of Engineering, University of Warwick, Coventry, CV4 7AL, UK

Abstract

In this paper theoretical and experimental studies are carried out to investigate the intrinsic relationship between tool flank wear and operational conditions in metal cutting processes using carbide cutting inserts. A new flank wear rate model, which combines cutting mechanics simulation and an empirical model, is developed to predict tool flank wear land width. A set of tool wear cutting tests using hard metal coated carbide cutting inserts are performed under different operational conditions. The wear of the cutting inset is evaluated and recorded using Zygo New View 5000 microscope. The results of the experimental studies indicate that cutting speed has a more dramatic effect on tool life than feed rate. The wear constants in the proposed wear rate model are determined based on the machining data and simulation results. A good agreements between the predicted and measured tool flank wear land width show that the developed tool wear model can accurately predict tool flank wear to some extent.

Key words: Metal cutting, carbide cutting insert, flank wear, wear model

* Correspondence to: Mr. Xichun Luo, School of Technology, Leeds Metropolitan University, Calverley Street, Leeds 1
LS1 3HE, UK   Tel: 0113-283 2600 ext: 3925 Fax: 0113 283 3110 E-mail: xichunluo72@hotmail.com

1. Introduction

Carbide cutting inserts are used extensively in metal cutting. The economical benefits of using carbide cutting inserts can be offset by rapid tool wear or premature tool failure if they are not used properly. Flank wear is a major form of tool wear in metal cutting. Tool flank wear is found to have detrimental effects on surface finish, residual stresses and microstructural changes in the form of a rehardened surface layer (often referred to as white layer) [1]. Therefore tool flank wear land width

* Correspondence to: Mr. Xichun Luo, School of Technology, Leeds Metropolitan University, Calverley Street, Leeds 2
LS1 3HE, UK   Tel: 0113-283 2600 ext: 3925 Fax: 0113 283 3110 E-mail: xichunluo72@hotmail.com

is often used to characterize the tool life. Some work on tool wear focused on prediction of tool wear by empirical modeling methods [2], time series methods [3], frequency domain analysis [4], pattern recognition and statistical methods [5], and hidden markov model method [6] for tool wear monitoring. These studies have gained various degrees of success in tool wear modeling although lots of experimental data are needed. More recently, artificial neural network and their combination with fuzzy logic models have been extensively applied to the area of tool wear estimation [7]. They have the advantages of superior learning, noise suppression, and parallel computation abilities. However the successful implementation of neural network strongly depends on proper selection of the type of network structure and amount of training data [6].

This research aims to develop a new flank wear rate model for more effectively and accurately predicting tool flank wear land width with minimum cost. The new model is based on the cutting force, cutting temperature simulation and an empirical model. The wear constants are calibrated by a set of tool wear cutting tests. The new tool wear rate model is also evaluated by the cutting tests.

2. Tool flank wear rate model

2.1 Modeling of interactions between cutting tool and workpiece

In metal cutting, tool flank wear is strongly influenced by the interactions between cutting tool and workpiece in the form of contact stress and cutting temperature. The interactions in turn depend on operational conditions, tool and workpiece material properties and cutting tool geometry. Therefore modeling of interactions between cutting tool and workpeice becomes the first task in the development of new tool flank wear rate model.

The theoretical orthogonal cutting model is adopted in this research for simplification. In orthogonal cutting, the tool tip is assumed sharp and the deformation is two-dimensional, i.e. no side spread [8].

From these conditions a force diagram as shown in Fig. 1 is constructed [8]. The resultant cutting force (F_R) can be expressed in terms of shear stress, friction and shear angle, width of cut, and uncut chip thickness:

$$F_R = \frac{F_s}{\cos(\phi_c + \beta_\alpha - \alpha_r)} = \tau_s bh \frac{1}{\sin\phi_c \cos(\phi_c + \beta_\alpha - \alpha_r)} \tag{1}$$

where τ_s, φ_c, α_r and β_a are shear yield stress on the shear plane assumed uniform over this plane, shear angle, tool rake angle and friction angle respectively. The friction angle is considered to represent the friction angle between tool and chip. It equals to the angle between the resultant force and the normal to the rake face. h and b are uncut chip thickness and width of cut respectively.

According to Fig. 1, the tangential and normal cutting forces can then be expressed in terms of the resultant force:

$$\left.\begin{aligned} F_t &= F_R \cos(\beta_\alpha - \alpha_r) \\ F_f &= F_R \sin(\beta_\alpha - \alpha_r) \end{aligned}\right\} \tag{2}$$
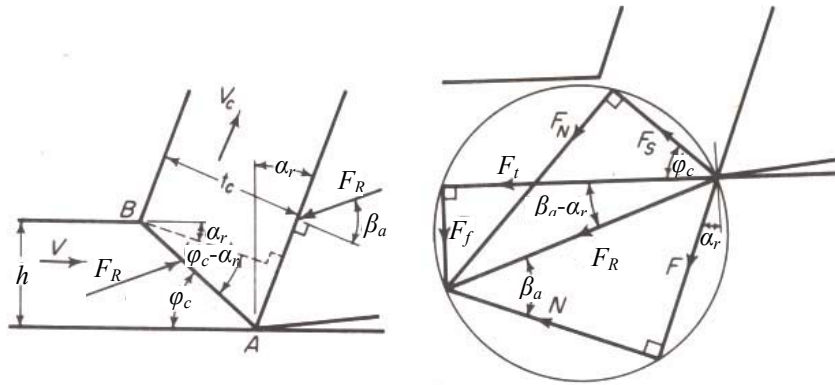

Fig. 1 The diagram of cutting forces [8].

Substituting Eq. (1) into Eq. (2), we can find the tangential and normal cutting forces as functions of tool geometry and the cutting conditions (i.e. uncut chip thickness (h) and width of cut (b) and process- and material-dependent terms (τ_s, β_a, φ_c, α_r):

$$F_t = b(t)h(t)[\tau_s(t)\frac{\cos(\beta_\alpha - \alpha_r)}{\sin\phi_c\cos(\phi_c + \beta_\alpha - \alpha_r)}$$
$$F_f = b(t)h(t)[\tau_s(t)\frac{\sin(\beta_\alpha - \alpha_r)}{\sin\phi_c\cos(\phi_c + \beta_\alpha - \alpha_r)}$$

(3)

In metal cutting the regenerative vibration and chip formation will change the uncut chip thickness, width of cut and shear stress of the work material respectively. They are expressed in functions of time (t). The detail of those modeling formulations can be found in the author's published paper in reference [9].

The heating resulted from flank-workpiece friction can be regarded as an elliptical shape heat source with uniform heat flux distribution. The temperature rise is given by:

$$\Delta T_f = \frac{2qa_i}{k_1\sqrt{\pi(1.273S_e + P_{e1})}}$$

(4)

where ΔT_f is the temperature rise in the tool flank – workpiece zone. q is the rate of heat supply per unit area. a_i is flank-workpiece contact length. k_1 and P_{e1} are thermal conductivity and Peclet number of the workpiece material [10] respectively. The normal cutting force and temperature will be inputs to an empirical tool wear rate model described below.

2.2 Tool flank wear rate model

Generally speaking, tool flank wear is caused by the friction between the flank face of the tool and the machined surfaces. Its wear mechanism is very complex. At the tool flank-workpiece surface contact area, tool particles adhere to the workpiece surface and are periodically sheared off. Adhesion of the tool and workpiece increases at higher temperatures. Adhesive wear occurs when hard inclusions of work material or escaped tool particles scratch the flank and workpiece as they move across the contact area as well. Abrasive/adhesive wear rate can be modeled as [11]:

$$\frac{dw}{dt} = \frac{A}{H}\sigma_n V_s$$

(5)

where w is flank wear land width. H, V_s and σ_n are hardness of the cutting tool material, sliding speed and normal stress between tool flank face and workpiece. A is abrasive/adhesive wear constant.

Although adhesive and abrasive wear mechanisms are predominant in flank wear, some diffusion wear also exists [12]. The tool wear rate model which considers diffusive wear is expressed as [12]:

$$\frac{dw}{dt} = B \exp(\frac{-E}{RT_f}) \tag{6}$$

where E, R and T_f are process activation energy, universal gas constant and cutting temperature in the tool flank zone respectively. B is diffusive wear constant.

Considering the complexity of tool flank wear mechanism, an empirical model, combining Eq. (5) and Eq. (6), is then used to calculate the tool flank wear rate. It is expressed as:

$$\frac{dw}{dt} = \frac{A}{H_t} \frac{F_f}{Vf} V_s + B \exp(\frac{-E}{RT_f}) \tag{7}$$

where V and f are cutting speed and feed rate respectively. They are used to calculate normal stress at tool flank/workpiece interface. The wear constants will be determined by the following calibration cutting tests.
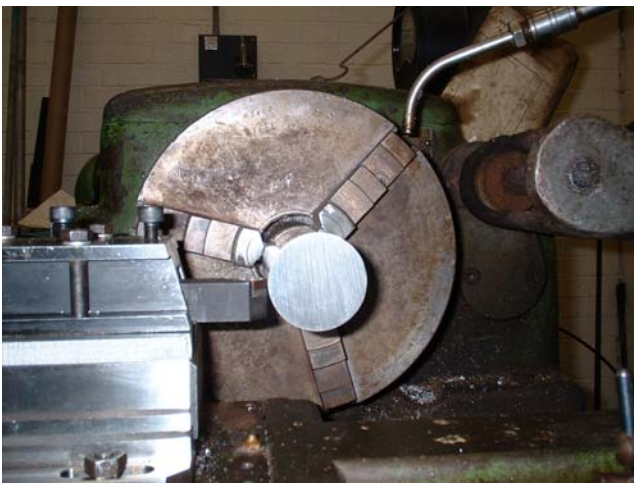

Fig. 2 Experimental setup.

3. Tool wear cutting test design

The purpose of cutting test is to determine the wear constants in Eq. (6) and evaluate the modeling approach. The facilities in the experimental study include machining system – lathe (Dean Smith & Grace Engine), cutting tool, and surface measurement equipment – Zygo New View 5000 microscope. The experimental

setup is illustrated in Fig. 2. The spindle speed of the lathe can vary from 250 rpm to 1400 rpm continuously. Hard metal (WC-TiC) coated carbide cutting inserts are used as the cutting tools. The cutting insert geometry is an 80° diamond shape with clearance angle of 7°. A group of cylindrical turning of low-alloy steel bars (Hardness 180 HB Φ 50 mm diameter) is performed at the conditions listed in Table 1. In the cutting tests cutting speed and feed rate are set at three difference levels, namely high, medium and low value. The test procedure consists of 20 cuts 20 mm in length, each at a decreasing diameter. Tool inspections are made at regular intervals with an optical microscope - Zygo New View 5000 microscope, which uses white light interferometry to produce images of surface topography. The tool wear land widths are measured through section profile of the cutting edge by the aid of Zygo's powerful image processing software - MetroPro. The measured results are used to determine the wear constants in Eq (7) and evaluate the modeling approach.

Table 1 Operational conditions in the tool wear cutting tests.

Test number	Cutting speed (m/min)	Feed rate (mm/min)	Depth of cut (mm)
1	76.93	0.3175	0.1
2		0.1588	
3		0.0794	
4	111.47	0.3175	
5		0.1588	
6		0.0794	
7	219.8	0.3175	
8		0.1588	
9		0.0794	
10	155.43	0.3175	
11	98.91	0.3175	

4. Wear constants validation and model evaluation

4.1 Tool flank wear

Fig. 3 shows the image of the cutting edge after 10 cuts in test No.1 from Zygo microscope, where the flank land is clearly visible on the worn cutting edge. As illustrated in Fig. 4, the flank wear width of 6.2 μm, can be measured from the two-dimensional profile section of the cutting edge. The preset tool life criterion is that when maximum flank wear width becomes equal of greater than 0.2 mm, the tool life ends.
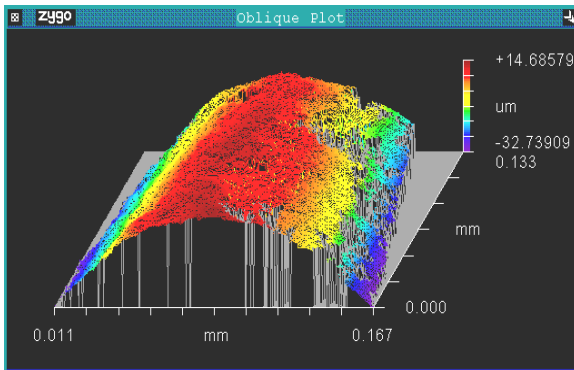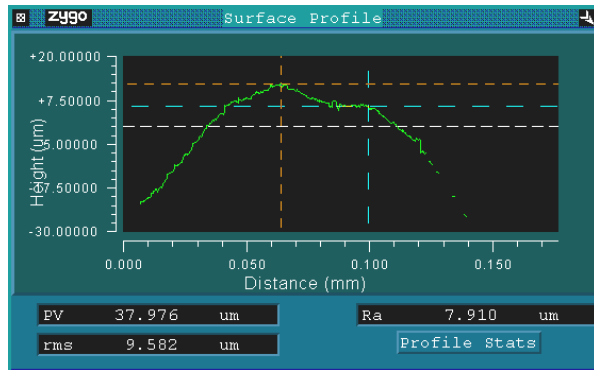

Fig. 3 Tool flank wear land image.

Fig. 4 Profile section of the cutting edge.

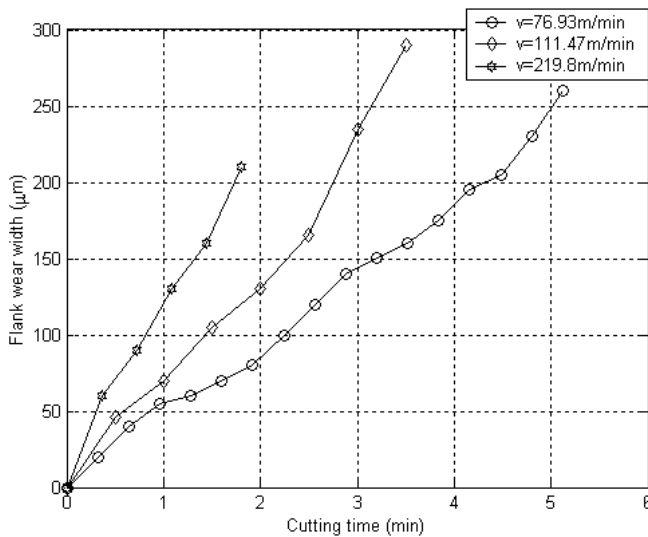Fig. 5 and Fig 6 present the measured flank wear widths against cutting time under different cutting speed and feed rate respectively. The clear observation in Fig. 5 is that tool life improved dramatically at condition that had a cutting speed of 76.93 m/min instead of 219.8 m/min. As shown in Fig. 6 the effect of feed rates on tool life is not so significant compared with cutting speed although it shows

Fig. 5 Flank wear land width against cutting time. (f = 0.1588 mm/rev).

the improvement of tool life with the decreasing of feed rate. Future work is required to investigate if an optimal cutting speed exits.
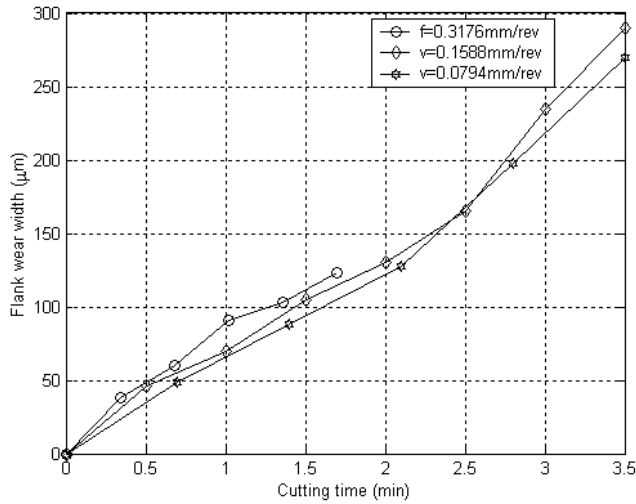

Fig. 6 Flank wear land width against cutting time under different feed rate ($V = 111.47$ m/min).

4.2 Determination of wear constants

In order to determine the wear constants in Eq. (7), 9 simulations are run to calculate the normal cutting force and temperature rise at tool-flank wear according to Eq.(3) and Eq. (4). The simulation is implemented in Matlab Simulink. The detail can be found in the author's published paper in reference [13]. The simulation results are input to Eq (7). The wear constants A and B are then acquired by regression analysis, which are 0.468 and 97.8 mm/min respectively.

4.3 Evaluation of tool wear rate model

The evaluation of the tool wear rate model is carried out by calculation of tool flank wear land width based on the developed flank wear rate model. Two cutting simulations are performed under the operation conditions of cutting test 9 and 10. The simulation results combine wear rate model to
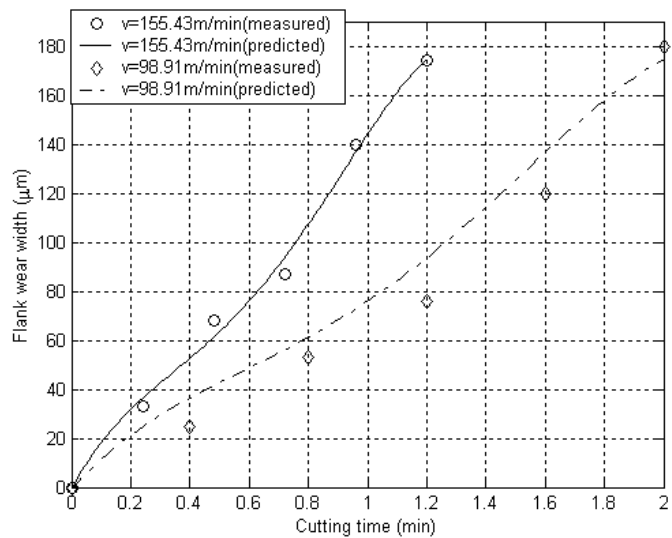

Fig. 7 Comparison of predicted and measured flank wear land width ($f = 0.3175$mm/rev).

calculate flank wear land width. Fig. 6 shows the comparison of the predicted and measured flank wear land width when cutting speed of 155.43 m/min and 98.91m/min are adopted. The observed good agreement between the predicted and measured values illustrates the proposed model can accurately predict the tool flank wear width to some extent.

5. Conclusions

The flank wear rate of carbide insert in metal cutting is predicted by a new model which combined cutting mechanics simulation and an empirical function. The wear constants of the wear rate model are determined from calibration a set of tool wear cutting test in conjunction with cutting simulations. Results of the tool wear cutting test indicate that cutting speed has a more dramatic effect on tool life than feed rate. Future work is required to investigate if an optimal cutting speed exits. The comparison of predicted and measured flank wear land width shows that the developed flank wear rate model can accurately predict tool flank wear land width to some extent.

References:

[1] T. G. Dawson and T. R. Kurfess, Wear trends of PCBN cutting tools in hard turning, http://www.hardinge.com/hardturn/PDF/Dawson_Metz_Paper.pdf, (Access on 1 March 2004).

[2] D. K. Born and W. A. Goodman, An empirical survey on the influence of machining parameters on tool wear in diamond turning of large single-crystal silicon optics, Precision Engineering, 25 (2001) 247-257.

[3] S. Y. Liang and D. A. Dornfield, Tool wear detection using time series analysis of acounstic emission, Transactions of the ASME: Journal of Engineering for Industry, 111(1989) 199-204.

[4] T. I. EI-wardany, D. Gao and M. A. Elbestawi, Tool condition monitoring in drilling using vibration signature analysis, International Journal of Machine Tools & Manufacture 36 (1996) 687-911.

[5] W. B. Lee, C. F. Cheung, W. M. Chiu and L. K. Chan, Automatic supervision of tool wear using pattern recognition analysis, International Journal of Machine Tools & Manufacture, 37 (1997) 1079-1095.

[6] L. Wang, M. G. Mehrabi, E. K. Jr, Hidden Markov model-based tool wear monitoring in turning, Transactions of the ASME: Journal of Manufacturing Science and Engineering, 124 (2002) 651-658.

[7] R. J. Ruo and P. H. Cohen, Intelligent tool wear estimation system through artificial neural networks and fuzzy modeling, Artificial Intelligent Engineering, 12 (1998) 229-242.

[8] E. J. A. Armarego and R. H. Brown, The Machining of Metals, Prentice-Hall, Inc., Englewood Cliffs, New Jersey, 1969, p.38-39.

[9] X. Luo and K. Cheng, Nonlinear effects in precision machining of engineering materials, Proceedings of 18th American Society of Precision Engineering Annual Meeting, pp. 489-493, 2003.
[10] T. H. C. Childs, K. Maekawa and P. Maulik, Effects of coolant on temperature distribution in metal machining, Material Science Technology, 4 (1988) 1006-1019.

[11] T. H. C. Childs, K. Maekawa, T. Obikawa and Y. Yamane, Metal Cutting: Theory and Applications, Arnold, London, 2000, p.77.

[12] C. Schmidt, P. Frank, H. Weule, J. Schmidt, Y. C. Yen and T. Altan, Tool wear prediction and verification in orthogonal cutting, Proceeding of 6th CIRP International Workshop on Modeling of Machining Operations, Hamilton, Canada, May 20, 2003.

[13] X. Luo, K. Cheng, R. Ward and R. Holt, A simulated investigation on surface texture/topography generation in precision turning processes, Proceedings of 34th International MATADOR Conference, 2004.

Nomenclature

A   abrasive/adhesive wear constant

B   diffusive wear constant

E   process activation energy

F_f	normal cutting force
F_R	resultant cutting force
F_t	tangential cutting force
H	hardness of cutting tool material
P_{el}	Peclet number of the workpiece material
R	universal gas constant
T_f	cutting temperature in the tool flank zone
V	cutting speed
V_s	sliding speed
w	flank wear land width
a_i	flank-workpiece contact length.
b	cutting width
f	feed rate
h	uncut chip thickness
k_1	thermal conductivity
q	rate of heat supply per unit area
α_r	tool rake angle
β_a	friction angle
τ_s	shear yield stress
φ_c	shear angle
σ_n	normal stress between tool flank face and workpiece
ΔT_f	temperature rise in the tool flank – workpiece zone